

Numerical modelling of the laser cladding process using a dynamic mesh approach

E.H. Amara*, F. Hamadi, L. Achab, O. Boumia

Laser Material Processing Group

Centre for Development of Advanced Technologies-CDTA

Po. Box 17, Baba-Hassen, Algiers, Algeria

* Corresponding author: E-mail address: amara@cdta.dz

Received 15.11.2005; accepted in revised form 15.02.2006

Analysis and modelling

ABSTRACT

Purpose: In this paper, a tridimensional modelling of laser cladding by powder injection is developed.

Design/methodology/approach: In our approach, the task consists in the numerical resolution of the governing equations including heat transfer and flow dynamic assuming an unsteady state. The related differential equations are discretized using the finite volume method, allowing to obtain an algebraic set of equations. The clad formation is simulated by considering the finite volume mesh deformation.

Findings: The shape of the deposited layer is determined as a function of the operating parameters related to the laser beam, the powder, the sample, and the environing atmosphere.

Research limitations/implications: By including as much as possible of terms describing physical mechanisms in the general form of the equations, one can model more accurately the cladding process. Afterwards, a validation with experimental results must be done.

Practical implications: The comprehension of the occurring physical processes would allow the enhancing of the products quality, the process can then be optimized since predictions on the results to be obtained can be made for given operating parameters.

Originality/value: In our contribution, the introduction of the dynamic mesh method involving the use of user defined functions (UDF) in the calculation procedure, have allowed to follow the variation of the cells volume and then to obtain the clad profiles as a function of the operating parameters.

Keywords: Numerical techniques; Laser cladding; 3D modelling; Finite volume method; Dynamic mesh

1. Introduction

The high precision industry is in constant need of metallic workpieces with exceptional characteristics [1-4]. To obtain an efficient behaviour of a workpiece submitted to different solicitations at its interface (extension, bending), it must present simultaneously features of high hardness, mechanical resistance, and ductility. These features can be obtained by surface treatment processes, with a goal to modify and enhance the workpiece surface hardness, and resistance to the corrosion [3], without weaken its internal properties of ductility.

The use of laser beams issued from high power laser devices for this kind of treatments constitutes the most interesting option

because of the possibilities offered by laser beams from the point of view of treatment accuracy, and collateral damages reduction [5-9].

Therefore, in the metallurgical applications field, laser surface treatment plays a great part, since it is by applying localized treatments, that high performance multi-materials can be realized. For instance, complex components like turbine blades or an engine valves can be laser treated by refusion or by cladding [8,10]. In the cladding process, the aim is to deposit a given thickness of an additional material layer on the workpiece. A clad can be obtained by injecting particles of the deposited material, in the form of powder, on the melted bath created by the moving laser beam on the surface substrate. Currently, the laser cladding by powder injection process is one of the advanced techniques of laser

material processing for surface treatment [11,12]. It is mainly used in restoring corroded work-pieces, in coatings of material with different properties on substrates, and in the fast conception of metallic prototypes. As shown on figure (1), a metallic sample is submitted to a powerful laser beam, while powder is injected over the melted bath to form after solidification a layer called the clad. Large regions, greater than the laser beam diameter can be covered by performing successive overlapping tracks. Contrary to refusion, the cladding process control is difficult because of the interactions between the laser beam, the powder particles and the melted regions. Indeed, even if the greater part of the laser power reaches the workpiece, a fraction is captured by the powder particles, which are thus heated. And only the powder particles that strikes the melted bath are then stucked, whereas the particles that strikes the solid region undergoe a ricochet and are then lost. Another complex phenomenon is the workpiece absorption modification (i.e., the ratio of the available laser power on the workpiece surface over the absorbed laser power by the workpiece [13]) following the shape of the melted region. Finally, because of the clad complex geometry that is presented under the laser beam, it is difficult to predict the laser power that minimize the remelted depth inside the workpiece, but still continue allowing the melting of the incident powder.

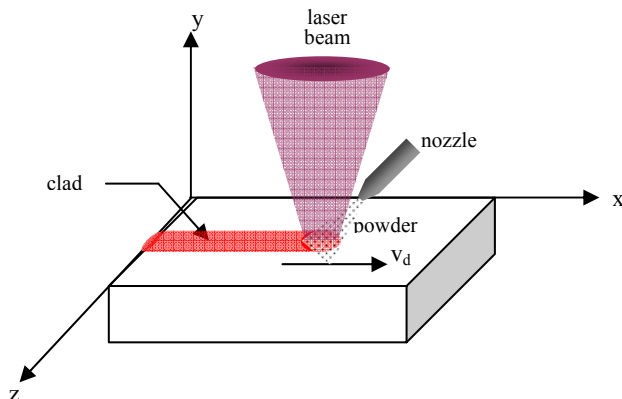


Fig. 1. Principle of laser cladding by powder injection.

Currently, modelling is an efficient mean used to optimize processes, since it allows to save time and investment [14-16]. Till the end of the 90's, few models dealing with laser cladding have been proposed. In the bidimensional (2D) situation, the complex shape of the melted zone is calculated by discretizing approaches like finite element or finite volume methods. In some models, the energetic equilibrium is assumed and the injected powder is supposed to be melted uniformly inside the melted bath, whereas in other models, the movement of the fluid inside the liquid is also considered, but the powder is supposed to melt instantaneously as soon as it reaches the melted bath. These models are not complete since they don't take into account the interactions between the powder particles as it crosses the laser beam, the modification of the absorption due to the melted bath shape, or the tridimensional (3D) aspects of the process. Furthermore, they are very complex from the numerical point of view and their conception is devoted to specialists.

In our contribution, a 3D modelling of laser cladding process is proposed. The physical phenomena produced in the processing zone are essentially the heat conduction, the Marangoni thermocapillary flow [17], the interaction between the powder and the melt bath, the mass transfers and diffusion, the laser-powder interaction, and the laser-work-piece interaction. The goal of our work is to predict the clad geometry by calculating its height and width. The adopted approach is the numerical solving of the heat conduction and the flow dynamic equations associated to suitable boundary conditions. The numerical approach allowed to obtain results using the finite volume discretization [18] implemented in the computational fluid dynamic CFD/ Fluent softwares [19]. And since the standard version of Fluent cannot take into account all the situations that could characterize a given problem, to deal with our specific one, our methodology is mainly based on the elaboration of procedures called UDF (user defined function), which are hooked to Fluent procedure when they are called for insertion in the calculation. But before start running the processor Fluent which solves the equations describing our problem for given boundary and initial conditions, the geometry of the workpiece is generated in the pre-processor Gambit. The choice of mesh and the boundaries are also determined in the Gambit stage. As the finite volume resolution of the equations is achieved, a post-processing allows the visualization, and the exploitation of the results. By using this approach, we have obtained the spatio-temporal evolution of the temperature field on the sample surface. The workpiece material is iron, which is irradiated by a laser beam issued from Nd-YAG device, assuming a Gaussian shape for the spatial distribution of beam energy. The determination of the local laser energy distribution by taking into account the shielding due to the powder projection, and the deduced local parameters, is used to calculate the profile of the reloaded material on the substrate. In this paper, the main contribution beside the elaborated UDF's, is the introduction of the dynamic mesh deformation technique. The obtained results allow us to observe the clad formation as a function of the processing parameters involving the beam displacement speed and its power, the powder injection geometry, the work-piece properties and the environing atmosphere.

2. Mathematical model

A laser beam with spatial gaussian distribution strikes on the surface of a metallic sample at $t=0$. As shown on figure (2), the laser or the work-piece displaces at relative speed v_d called the process speed. By powder injection, a layer constituted of reloaded material is formed on the substrate to generate what is called the clad.

The temperature distribution $T(x,y,z,t)$ is obtained by solving the 3D heat conduction equation:

$$\frac{\partial(\rho C_p T)}{\partial t} + \nabla \cdot (\rho C_p v_d T) - \nabla \cdot (K \nabla(\rho T)) = Q \quad (1)$$

where Q is the generated power in unit volume of substrate, est la puissance g n r e par unit  de volume du substrate, K is the material heat conductivity, C_p its specific heat capacity sp cifique, ρ its density, t the time, and v_d the process velocity.

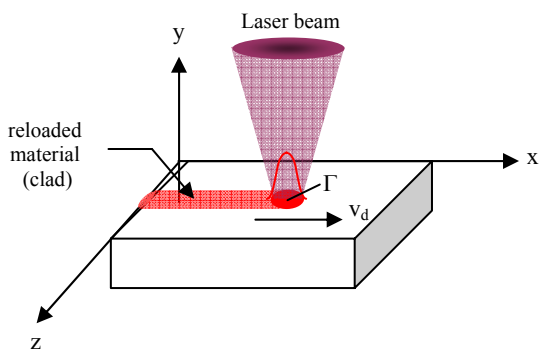


Fig. 2. The clad formation

2.1. Initial and boundaries conditions

The absorption by the workpiece of the laser beam energy falling on the treated surface is considered. The total power absorbed on the sample surface is noted P_w , and the thermal convection and radiation losses are taken into account on the processed and the non-processed regions. Therefore, the boundaries conditions are written as :

$$-K(\nabla T \cdot \vec{n})_{\Omega} = \begin{cases} P_w - h_c T - \epsilon \sigma (T - T_a)^4 & \Omega \in \Gamma \\ -h_c T - \epsilon \sigma (T - T_a) & \Omega \notin \Gamma \end{cases} \quad (2)$$

where \vec{n} is the surface normal vector, h_c the convection heat transfer coefficient, ϵ the surface emissivity, σ the Stefan-Boltzmann constant ($5.67 \cdot 10^{-8} \text{ W/m}^2 \text{ K}^4$), Ω the surfaces of the work-piece, and Γ the part of surface that is reached by the laser beam at a given instant t .

Following the relation given by Yang [20], we have assumed in our modelling, that we can consider a combined coefficient h_c to take into account both the convective and the radiative losses, such as:

$$h_c = 24.1 \times 10^{-4} \epsilon T^{1.61} \quad (3)$$

This form of expression of the heat losses by convection and radiation allows beside the simplification of the equations, to save a calculation time. For the iron, we take $\epsilon = 0.4$.

The initial conditions that should be satisfied are:

$$T(x, y, z, t=0) = T_a \quad (4)$$

where T_a is the ambient temperature taken to be equal to 300 K. Moreover, when the time becomes important relatively to the process time scale, we consider that the temperature distribution inside the workpiece becomes at the ambient conditions such as:

$$T(x, y, z, t \rightarrow \infty) = T_a \quad (5)$$

2.2. The effective power absorbed by the work-piece

The modelling of laser cladding process requires the comprehension of coupled mechanisms which are mainly the attenuation of a part of the laser beam by the powder particles. Indeed, the absorbed laser power by the workpiece results from the fact that before the laser beam reaches the surface of the workpiece, it crosses the powder flux which reduces a part of the energy which goes in powder particles heating. Subsequently, the powder flux can either enter in the melted part of the workpiece or undergo a ricochet. The other mechanisms are related to the workpiece absorption which vary as a function of the melted zone shape. The last depends on the laser energy distribution at the workpiece surface.

Following Picasso *et al.* [21], the total quantity of absorbed power P_w by the work-piece relatively to the laser beam supplied power is given after considering the effect of beam attenuation due to the powder shielding. The effective power absorbed by the work-piece is:

$$P_w = P_1 \left\{ \beta_w \left(1 - \frac{P_{at}}{P_1} \right) + \eta_p \beta_p \frac{P_{at}}{P_1} \left[1 + (1 - \beta_w) \left(1 - \frac{P_{at}}{P_1} \right) \right] \right\} \quad (6)$$

Where P_{at} is the attenuated power, and P_{at}/P_1 corresponds to the attenuation term which represents the ratio of the projected area representing the particles of powder shadows relatively to the laser area. This ratio can be determined starting from simple geometric considerations, by assuming that the laser beam and the powder flux are two crossing cylinders, and that the shadows produced by a given powder particle on another particle or more powder particles are neglected. This assumption is reasonable since the volume fraction of powder in the gas jet carrying the particles, is generally smaller than 1%. The particles of powder absorb a part of the attenuated power and restore it to workpiece unless they strike and penetrate the melted bath. As described in reference [21], β_p represents the powder gas jet absorption and η_p the powder efficiency. Toyerskani *et al.* [22] suppose that at the workpiece surface, the absorption of a laser beam which section is circular, depends on its inclination relatively to the surface of the workpiece. Depending on the inclination angle θ , the term β_w which represents the workpiece surface absorption, is given as:

$$\beta_w(\theta) = \beta_w(0) (1 + \alpha_w \theta) \quad (7)$$

where $\beta_w(0)$ represents the absorption of a plane surface relatively to the laser beam.

The reflected power at the surface workpiece is important, as it is the case when a CO_2 laser beam is used, and it is also attenuated by the incident particles of powder which absorb a part of the reflected power. The portion of reflected power that is transferred to the workpiece by the particles of powder is then :

$$\eta_p \beta_p (1 - \beta_w) P_1 \left(1 - \frac{P_{at}}{P_1} \right) \frac{P_{at}}{P_1} \quad (8)$$

This expression constitutes a part of the right hand term in the expression of the effective absorbed power given in the equation (6).

2.3. Effect of the Marangoni thermocapillary convection

During the laser cladding process, the heat diffusion occurs by two main mechanisms: the heat conduction, and the Marangoni thermocapillary flow. The melt bath movement effects due to the thermocapillary phenomena could be taken into account by considering a modified heat conductivity. This allows to calculate the melt bath frontiers, and generally as it was suggested by Lampa *et al.* [17] following experimental observations, the occurrence of a thermocapillary flow is induced by a heat conductivity at least equal to twice the value of that in the case of a stationary melt bath. This increasing could be expressed by :

$$K^*(T) = a K(T_m) \quad \text{if } T > T_m \quad (9)$$

where $a = 2.5$ is the correction factor and K^* the modified heat conductivity.

2.4. Dependence of the physical properties on the temperature

In our modelling, the material physical properties such as the density, the heat capacity and the heat conductivity are considered to vary with the temperature, and their expressions are deduced starting from the Duley [23] reported data concerning the iron, as shown on table (1).

Table 1.

T (K)	K (W/m/K)	C_p (J/kg/K)	κ (m^2/s)
273	83.5	420	$2.8 \cdot 10^{-5}$
500	61.5	540	$1.54 \cdot 10^{-5}$
1000	32.5	980	-
2000	42.5	-	-

where κ , representing the material heat diffusivity, allows to obtain the density at different temperatures, having the heat conductivity, the heat capacity and the heat diffusivity which are related by the equation:

$$K = \frac{\kappa}{\rho C_p} \quad (10)$$

An expression is deduced for these quantities as a function of the temperature such as:

$$\rho(T) = -0.4522 T + 7755.7 \quad \text{in } [kg/m^3] \quad (11)$$

$$K(T) = -0.0218 T + 76.307 \quad \text{in } [W/m/K] \quad (12)$$

In the computing procedure, when the temperature becomes higher than the fusion temperature, the effect of the Marangoni

thermocapillary starts and the equation (12) is automatically switched to equation (9).

To take into account the latent heat effects on the temperature distribution, an increasing of the heat capacity given by Toyerskani *et al.* [22] is applied such as :

$$C_p^*(T) = \frac{1}{T_m - T_a} \left[L_f + \int_{T_a}^{T_m} C_p dT \right] \quad (13)$$

where L_f is the material latent heat of fusion ($L_f = 2.76 \cdot 10^5$ J/kg for the iron), and C_p^* the modified heat capacity. By developing the expression (13), we obtain an approximation of the heat capacity as a function of the temperature. The equation can then be written as a second order polynomial such as:

$$C_p^*(T) = 2.6137 \cdot 10^{-4} T^2 + 0.12034621 T + 124 \quad [J/kg/K] \quad (14)$$

3. Problem geometry and resolution

An iron parallelepipedal sample with the dimensions: 50 mm x 10 mm x 5 mm, is considered. On figure (3), the 3-D structured mesh used in our modelling is represented. It is constituted of : 23200 hexaedrons, about 8000 faces, and 27270 nodes. The problem geometry, the domain meshing and the boundary reservation are performed by the pre-processor GAMBIT of FLUENT softwares. At the first step an *.msh file provided by Gambit is used by the processor FLUENT to solve the corresponding equations by finite volume discretization. After obtaining the convergence, a post-processing is started to exploit and to present the results.

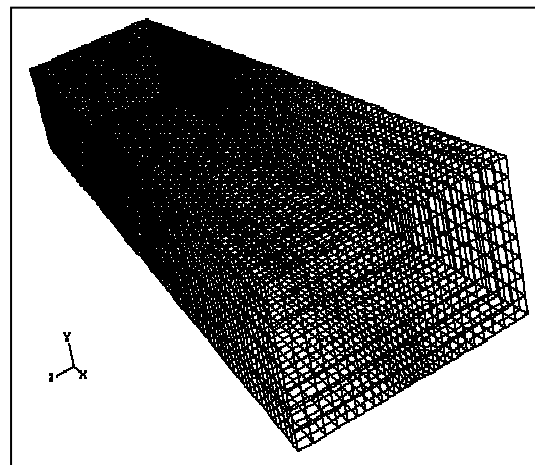


Fig. 3. Used finite volume mesh

A user-defined function, or UDF, written in C programming language, can be interactively loaded on the calculation procedure during the numerical resolution of the equations by the processor FLUENT. This allows to enhance the standard features

of the calculation code. Thus, the UDFs allow to customize FLUENT to adapt it for a particular need required by the modelling. They can be used in various applications such as customizing boundary conditions or the definition of workpieces physical properties depending on the temperature.

3.1. Implementation of a gaussian beam shape using an UDF

In our case, the developed laser cladding modelling considers a gaussian spatial distribution for the laser beam. In the standard version of FLUENT, the energy supply is introduced as a boundary condition representing the energy flux (W/cm²) which value is constant. To use a Gaussian energy distribution at the workpiece surface, the elaboration of a UDF is necessary. Considering the laser beam displacement on the workpiece, as it is represented on figure (4), we can distinguish on the workpiece surface the regions submitted to the laser radiation and those that are not exposed. The position of a face centre in the sense of finite volume is represented by the radius *r*. The last is given as a function of the position *z*₁ of the beam center relatively to the direction *z*, and of the laser beam travelled distance *L* = *v*_d *t*, at a displacement speed *v*_d following the *x* direction *x*, such as:

$$r^2 = (L-x[0])^2 + (z_1 - x[1])^2 \tag{15}$$

One can then locate the position of the face relatively to the focal spot by performing the instruction :

$$\text{if } (r \leq r_1) \quad \text{then} \quad I = A I_0 \exp (-2r^2/r_1^2) \tag{16}$$

else *I* = 0

where *r*₁ is the laser beam radius over the workpiece surface, *I* (W/cm²) the laser intensity or the irradiance, and *A* the material absorption coefficient.

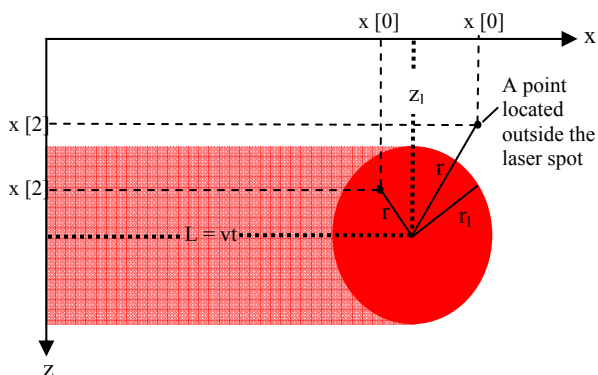


Fig. 4. Laser beam spot on workpiece surface

The elaborated UDF representing the laser energy deposited during the displacement is built from the macro DEFINE-PROFILE supplied with the FLUENT softwares. The aim of this

macro is to inject during the calculation, a boundary condition which vary in space and time. In the written UDF, we determine the faces composing the surface mesh, which are located inside the focal spot on given position and instant, through the coordinates *x*[0] and *x*[2] of the centroid or the face centre (of the control volume). We have also to precise that by convention, *x*[0] represents the projection of the point in the *x* direction, *x*[1] in the *y* direction, and *x*[2] in the *z* direction *z*. The data inserted in the UDF concern the laser power, the length and the width of the sample, the focal spot radius, the process or displacement speed, and the absorption coefficient of the material. In the iron case, considering a beam issued from a Nd-YAG laser device, the absorption coefficient is taken to be equal to 0.6.

3.2. Simulation of mesh deformation

The dynamic mesh model supplied by FLUENT code can be used to model flows where the shape of the domain is changing with time due to motion on the domain boundaries. The update of the volume mesh is handled automatically by FLUENT at each time step based on the new positions of the boundaries. To use the dynamic mesh model, one need to provide a starting volume mesh and the description of the motion of any moving zones in the model. FLUENT allows to describe the motion using either boundary profiles or UDFs. description of the motion to be specified on either face or cell zones is expected by FLUENT. If the model contains moving and non-moving regions, one need to identify these regions by grouping them into their respective face or cell zones in the starting volume mesh that is generated. Furthermore, regions that are deforming due to motion on their adjacent regions must also be grouped into separate zones in the starting volume mesh. The boundary between the various regions need not be conformal [19]. One can use the non-conformal or sliding interface capability in FLUENT to connect the various zones in the final model. Three mesh motion methods are available in FLUENT to update the volume mesh in the deforming regions subject to the motion defined at the boundaries: The spring-based smoothing, the dynamic layering , and the local remeshing

In our modelling, the dynamic mesh technique based on spring smoothing is used to follow the clad formation. Figure (5) shows at a given instant the mesh deformation as a function of the laser, the material, and the injected powder parameters.

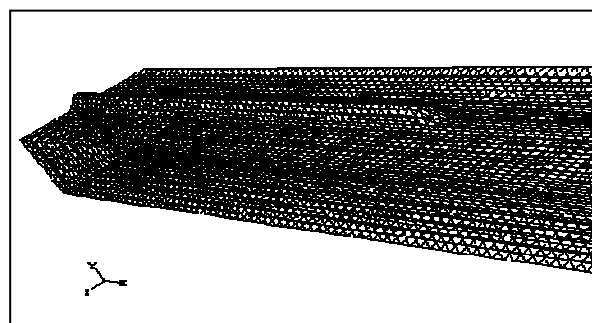


Fig. 5. Mesh deformation effect on the cells network

4. Results and discussion

The temperature field is first calculated in the case of a Gaussian profile of the spatial laser beam distribution. In the presented results, the variation of the physical properties of the material with temperature growing is considered.

In an UDF the mesh cells that are found inside the laser beam spot are identified by comparing cell's radius with the beam radius. The related laser intensity is then deduced.

On figure (6) sequences of temperature spatial distribution is shown in the case of an iron sample, irradiated by a continuous laser beam which power is 350 W and a spot radius of 1 mm. The displacement velocity v_d is taken to be equal to 2 mm/s.

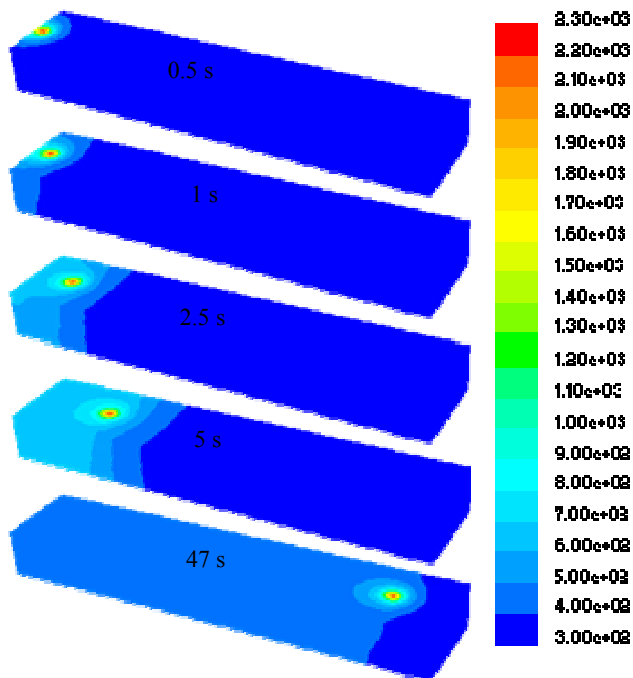


Fig. 6. Temperature distribution on iron sample

When the cladding process is considered, the clad formation can be obtained as a function of the laser beam, the material, and the injected powder parameters. The UDF which calculate the mesh deformation is elaborated using the dynamic mesh technique available with FLUENT softwares.

For a laser beam power of 350 W, a total effective absorbed power of 213 W is obtained, when a powder feedrate of $1.67 \cdot 10^{-3}$ kg/s, and a radius powder spray jet of $1.2 \cdot 10^{-3}$ m are considered. The powder material is assumed to be of same nature as the workpiece material, which means that in the case of iron, the powder density is equal to 7800 kg/m^3 . A laser spot radius is 1 mm, a process speed of 2 mm/s, a workpiece emissivity of 0.4, and an ambient temperature of 300 K are taken in the simulation of clad formation.

On figure (7), represent clad formation by powder of same nature as the substrate, for an effective absorbed power equal to 213 W, and a process velocity of 1 mm/s.

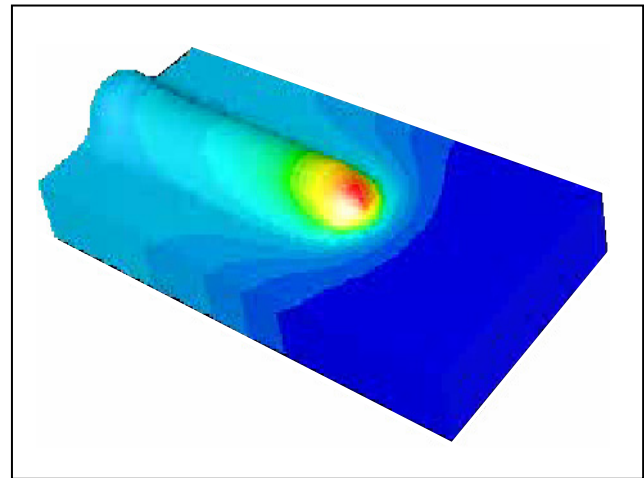


Fig. 7. Clad formation on iron sample by iron powder injection

The flexibility of the numerical modelling is required if it is intended to couple it with an industrial application like laser cladding. And as it was reported before, the use of UDFs allows to increase efficiently the performances of FLUENT calculation procedure to take into account effects of spatio-temporal changes in the operating parameters. One of the important parameters of laser cladding process is the displacement velocity of the laser beam relatively to the workpiece surface. To highlight this aspect in the present simulation, figure (8) shows the influence of the process speed on the height of the obtained clad. The laser beam parameters, powder injection features and material are the same as those taken to obtain the result presented on figure (7) it is remarked that obviously, more the velocity is higher, more the clad height is smaller.

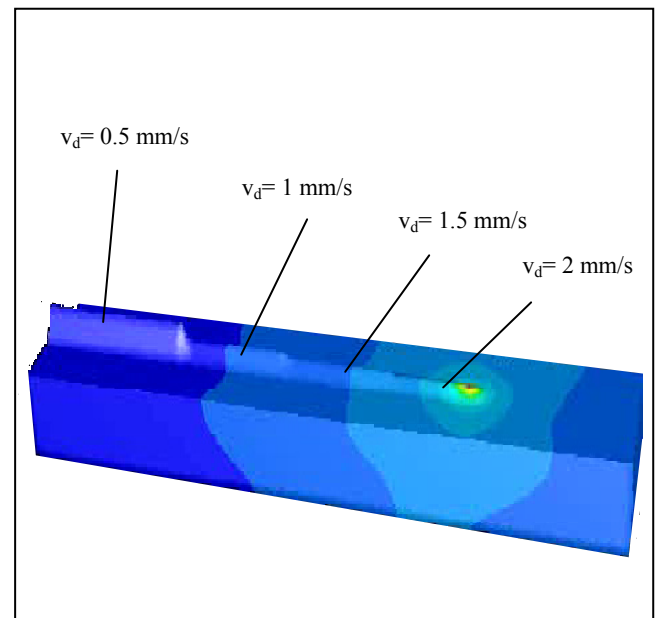


Fig. 8. Displacement velocity effect on clad height

5. Conclusion

The proposed modelling approach allows the simulation of clad formation over a metallic surface by laser beam-melt bath-powder interaction. The model offers the possibility of studying the influence of parameters related to the laser beam, the powder injection, the sample physical properties, and the environment.

References

- [1] B. Brenner, W. Reitzenstein, Laser Hardening of Turbine Blades, Industrial Laser Review, 1996.
- [2] N.Q. Wu, C. Xia, M. Li, N. Perrusquiva, S.X. Mao, J. Eng. Mat. Tech., Vol.126, (2004) 8-13.
- [3] L.Cunha, M. Andritshky, L. Rebouta, F. Vaz, Proc. 5th Int. Sci. Conf AMME'96, Poland (1996).
- [4] I. Schäffler, P. Geyer, P. Bouffieux, P. Delobelle, J. Eng. Mat. Tech., Vol.122, (2000) 168-176.
- [5] E.A.Werner,V.V. Siberschmidt, H.J. Böhm, J. Eng. Mat. Tech., Vol.125, (2003) 1-1.
- [6] K. Komvopoulos, K. Nagarathnam, J. Eng. Mat. Tech., Vol.112 (1990) 131-143.
- [7] S. Barnes, M.J. Nash, Y.K. Kwok, J. Eng. Mat. Tech., Vol.125, (2003) 327-377.
- [8] S. Atamert, H.K.D.H. Bhadeshia, Metall. Trans. A, Vol. 20A, (1989) 1037-1054.
- [9] L. Börjesson, L.E. Lindgren, J. Eng. Mat. Tech., Vol.123, (2001) 106-111.
- [10] G. Cai., G.Molino, Proc. Laser-6, (1990) 79-90.
- [11] B. Grünwald, Proc. ECLAT '92, (1992) 411-416.
- [12] J.A. Folkes, K. Shibata, J. of Laser Applications, Vol. 6, (1994) 88-94
- [13] G. Stern, Proc. ECLAT '90, (1990) 25.
- [14] J. Li, L. Yuan, Lasers in Engineering, Vol. 2, (1994) 239-245.
- [15] S. Finnie, W. Cheng, I. Finnie, J.M. Drezet, M. Gremaud, J. Eng. Mat. Tech., Vol.125, (2003) 302-308.
- [16] M. Mochizuki, M. Hayashi, T. Hattori, J. Eng. Mat. Tech., 122, (2000) 98-105.
- [17] C. Lampa, A.F.H. Kaplan, M. Resch, C. Magnusson, Lasers in Engineering, Vol.7 (1998) 241-252.
- [18] S. V. Patankar, D.B. Spalding, Int. J.of Heat and Mass Transfer, Vol.15, (1972) 1787
- [19] www.fluent.com
- [20] L. Yang, X. Peng, B. Wang, International Journal of Heat and Mass Transfer, Vol. 44 (1986) 4465.
- [21] M. Picasso, C.F. Marsden, J.D. Wagniere , A. Frenk, M. Rappaz, Metallurgical and Materials Transactions B, Vol. 25 (1994) 281-291.
- [22] E. Toyerskani, A. Khajepour, S. Corbin, ICALEO Proc., Scottsdale, Arizona, USA (2002).
- [23] W.W. Duley, CO₂ Lasers: Effects and Applications, Acad. Press, New York , 1976.